Applied Water Science (2019) 9:154
https://doi.org/10.1007/s13201-019-1035-4

ORIGINAL ARTICLE

Understanding the morphology of MWCNT/PES mixed-matrix membranes using SANS: interpretation and rejection performance

Km Nikita[3] · P. Karkare[3] · D. Ray[1] · V. K. Aswal[1] · Puyam S. Singh[2] · C. N. Murthy[3]

Received: 4 January 2019 / Accepted: 4 September 2019 / Published online: 13 September 2019

Abstract

We describe the relationship between the morphology and rejection performance by the mixed-matrix membranes as a unique class of high water flux nanofiltration membranes comprising polyethersulfone/functionalized multiwalled carbon nanotubes (PES/f-MWCNTs). These membranes contain aligned MWCNTs uniformly distributed inside a PES matrix prepared using conventional phase-inversion technique. The small-angle neutron scattering analysis confirmed the high porosity and uniformity among of the pores of CNTs in the membranes. The frictionless water transport from vertically oriented f-MWCNTs were verified to facilitate remarkable enhancement in the water flux through the membranes. The water transportation speed, as well as rejection, of selected heavy metals increases nearly about 3 times and 2–3.5 times, respectively, than the pristine PES membrane, depending upon CNTs loading. Low working pressure and good retention properties make these membranes to be an ideal for the application of highly efficient filtration units.

Keywords MMMs · MWCNTs · SANS · Morphology · High water flux

Introduction

There has been immense activity in the use of polymeric as well as ceramic membranes in the field of water treatment, but one of the disadvantages of these membranes are fouling, chemical and thermal less stability, low permeability and selectivity, and lower rejection of specific contaminants. Thus, the idea of membranes having both polymeric substrate as well as inorganic filler came in existence, which can overcome the above-mentioned limitations to a large extent. There are different studies having various fillers like Fe_3O_4 nanoparticles (Alam et al. 2013; Chan et al. 2015; Ghaemi et al. 2015; Bagheripour et al. 2016; Mondal et al. 2017), oxidized multiwalled nanotubes (Yin et al. 2013; Celik et al. 2011a, b), TiO_2 nanoparticles (Luo et al. 2005; Rahimpour et al. 2012; Esfahani et al. 2015; Mbuli et al. 2018; Farahani and Vatanpour 2018), functionalized MWCNT (Qiu et al. 2009; Liu et al. 2018; Benally et al. 2018; Ho et al. 2017; Lee et al. 2016), silver nanoparticles (Taurozzi et al. 2008; Zhang et al. 2012; Sonawane et al. 2017), modified silica nanoparticle (Farahani and Vatanpour 2018; Huang et al. 2017; Martín et al. 2016), chitosan/zinc oxide nanoparticles (Munnawar et al. 2017; Ahmad et al. 2017; Elizalde et al. 2018), beta cyclodextrin–polyurethane (Adams et al. 2014), graphene oxide (Ho et al. 2017; Chai et al. 2017; Karim et al. 2017; Mukherjee et al. 2016; Karkooti et al. 2018), manganese oxide and alumina nanoparticles (Delavara et al. 2017; Gohari et al. 2014), zeolites (Liu et al. 2014; Grabczyk et al. 2017; Amiri et al. 2017), attapulgite (Zhang et al. 2014), and fumed silica (Mavukkandy et al. 2017), which have reported good results with respect to flux and separation performance. However, the underlining changes in the membrane morphology have not been addressed adequately. Carbon nanotubes are promising materials as adsorbent as well as inorganic fillers for the membranes. Its chemical, thermal, and mechanical properties make it a prominent candidate in the field of membrane technology. In a study, carbon nanotubes coated with N-isopropylacrylamide hydrogel (NIPAM-CNT) was synthesized and was incorporated

✉ C. N. Murthy
chivukula_mn@yahoo.com

1 Solid State Physics Division, Bhabha Atomic Research Centre, Mumbai, India

2 Membrane Science and Separation Technology Division, Central Salt and Marine Chemicals Research Institute, Bhavnagar, India

3 Applied Chemistry Department, Faculty of Technology and Engineering, The Maharaja Sayajirao University of Baroda, Vadodara, India

into poly (ether-block-amide) for efficient CO_2 separation (Zhang et al. 2016). Yin et al. (2013) reported that in the hollow fiber membrane with composition of pristine and oxidized MWCNT-incorporated polysulfone membranes, the pure water flux gradually increases and then decreases with different polymer concentration having increasing weight percentages of fillers. Polyamide reverse osmosis (RO) membranes with carbon nanotubes (CNTs) were prepared by interfacial polymerization using trimesoyl chloride (TMC) solutions in n-hexane and aqueous solutions of m-phenylenediamine (MPD) containing functionalized CNTs. Here the effect of polymerization time and reaction temperature on dispersion of nanotubes was studied (Kim et al. 2014). Goh et al. (2013) have reviewed the transport properties and chemical functionalities of nanotubes to potentially facilitate excellent flux of water transport and the details regarding the utilization of CNT for desalination has been highlighted. MWCNT were also used to prepare thin film nanocomposite by interfacial polymerization of support layer containing modified nanotubes and thin film containing Ag nanoparticles. The study reveals that rejection of NaCl and Na_2SO_4 was same for thin film nanocomposite with and without silver nanoparticles though permeability and biofouling of the modified membrane was improved (Kim et al. 2012). This study does not show the role of the morphology of the membrane in the observed results. Heavy metals are one of the hazardous and major sources of pollutant in the wastewater and industrial effluents. Even very low concentration of these metals can cause severe health diseases. Precipitation, coagulation, ion exchange, and adsorption are some of the techniques which are frequently been used for the decontamination of heavy metal pollutants. However, membrane-based separations of these metals are becoming most efficient because of the cost-effectiveness, lesser energy consumption, thermal and mechanical stability, large surface area, and better selectivity (Delavara et al. 2017). Different studies are there in which mixed-matrix membranes are employed for the removal of heavy metals (Chan et al. 2015; Ghaemi et al. 2015; Mondal et al. 2017; Mbuli et al. 2018; Delavara et al. 2017; Hosseini et al. 2017; Gupta et al. 2015; Shah and Murthy 2013). However, there is no correlation between the membrane performance and the type of filler or the morphology. In our previous work, polysulfone/functionalized multiwalled carbon nanotube-dispersed mixed-matrix membranes were employed for the removal of cadmium, lead, arsenic, chromium, copper (Shah and Murthy 2013). The minimum weight percentage of nanotubes used there was 0.1%, and the results showed very high pure water flux though no detailed morphological studies were undertaken. To understand the morphological changes brought about by the addition of functionalized nanotubes, we have further decreased the multiwalled carbon nanotubes concentration to 0.05% weight and studied the effect of reduced concentration on pore dimension and porosity and compared with the neutron scattering studies to understand the morphology. Pure water flux and heavy metal removal parameters of polyethersulfone/functionalized multiwalled carbon nanotube-incorporated mixed-matrix membranes were compared with our earlier studies.

Experimental

Materials

Polyether sulfone (PES) Veradel 3300 was purchased from M/s Permionics Membranes Limited, Vadodara, India. MWCNTs (diameter 6–9 nm) were commercial sample from M/s Sigma-Aldrich, the surfactant Brij 98 (Sigma-Aldrich), ethylene diamine (> 99%, Sigma-Aldrich), and sodium azide (> 99%, Sigma-Aldrich) were used as received.

Functionalization of MWCNTs and membrane preparation

The functionalization of MWCNT and membrane preparation was described in our previous work (Shah and Murthy 2013). In brief, the commercial MWCNT was first purified to remove unwanted metals and soot. Carboxylic, azide, and amide functionality were attached to nanotubes in various steps. These functionalized fillers were dispersed in different weight percentage (0.05, 0.1 and 1) into the 18% polyethersulfone solution. The membranes were prepared using the dry–wet phase-inversion process.

Characterization

Functionalized CNT as well as the functionalized nanotube-incorporated polymeric membranes were analyzed by different analytical techniques. The codes for the different mixed-matrix membranes are mentioned in Table 1. Functionalized CNT was analyzed by FTIR and Raman spectroscopy to ensure the functionalization of nanotubes with different functionality (Shah and Murthy 2013; Mangukiya et al. 2016). The functionalized nanotubes as well as membranes were characterized by TGA to verify the thermal stability (Shah and Murthy 2013). The structural morphology of the membranes was checked by field emission scanning electron microscopy (FESEM). The porosity of membranes were analyzed by two different techniques: (1) Small-angle neutron scattering (SANS) and (2) mercury porosimetry. Permeation test were carried out to test the separation efficiency of the membranes.

Table 1 Sample details of the different MWCNT-incorporated polyether sulfone membranes

Functionalization of nanotube	MWCNT concentration (%)	Membrane code
–	–	M1
Oxidized	0.05	M205
Oxidized	0.10	M201
Oxidized	1.00	M21
Amide	0.05	M305
Amide	0.10	M301
Amide	1.00	M31
Azide	0.05	M405
Azide	0.10	M401
Azide	1.00	M41

Small-angle neutron scattering

The small-angle neutron scattering experiments were performed on SANS diffractometer at Dhruva Reactor, Mumbai, India (Aswal and Goyal 2000). The instrument utilizes a neutron velocity selector to get a monochromated neutron beam with a mean wavelength of 5.2 Å, with a wavelength resolution ($\Delta\lambda/\lambda$) of approximately 15%. The angular divergence of the incident beam was $\pm 0.5°$. The scattered neutrons were detected using a linear He^3 position-sensitive gas detector. The data were collected over the wave vector range ($Q = 4\pi \mathrm{Sin}\theta/\lambda$) of 0.015–0.35 $Å^{-1}$, where 2θ is the scattering angle and λ is the wavelength of incident neutrons. The diffractometer is well suited for the study of a wide variety of system having characteristic dimensions between 10 and 300 Å. The membrane samples was cut into small pieces of 1×1.5 cm dimension, and few pieces were put together in the aluminum foil and positioned in the path of the beam. The data analysis was done after the data were corrected for the direct beam and the background contribution (Pedersen 1997).

Mercury flow porosimeter

The pore dimensions of the membranes were also confirmed by mercury flow porosimeter, Pascal 400 Thermoquest, USA.

Field emission scanning electron microscopy

Morphological studies were made by field emission scanning electron microscopy (FESEM EDAX XL-30 Philips, Netherlands).

Contact angle measurement

Hydrophilicity of the membrane surface was measured by contact angle meter ACAMNSC 03, M/s Apex Instruments Pvt. Ltd. Deionized water was dropped onto membrane surface and contact angle was measured immediately. An average of seven readings was taken for each membrane.

Filtration performance

The permeation performance of the membranes was measured on a membrane filtration cell fabricated in-house. The effective membrane area used was 50 cm^2. Before starting the experiment, the membranes were stabilized for 2 h at 71 psi pressure. The pure water flux and rejection capacity for heavy metals of the membranes were obtained by performing the experiment. The rejection was calculated as given below:

$$R(\%) = \frac{C_f - C_p}{C_f} \times 100.$$

Here C_f and C_p are concentration of metal ions in feed and permeate, respectively, and were measured by atomic absorption spectroscopy (AAS) and also by conductivity bridge analyzer.

Results and discussion

Characterization of membranes

The FESEM micrograph of cross section of cold-fractured mixed-matrix membranes shows that the essential asymmetric nature of membrane is retained. It also shows the presence of functionalized nanotubes. The FESEM images of the mixed--matrix membranes clearly show the formation of finger like pores (Fig. 1a). One can see that CNTs appear toward the surface of the mixed-matrix membranes (Fig. 1b). As shown in Fig. 1c, an interconnected network of nanotubes exists inside the PES matrix. We consider that occurrence of CNTs perpendicular to the polyethersulfone matrix contribute to the enhancement in flux that will be discussed in detail in the following section.

Figure 2 shows the disparity between the contact angle of pristine polyethersulfone and f-MWCNT (oxidized, amide, and azide functional group)-incorporated mixed-matrix membranes. The contact angle of the pristine PES membrane is $73.3 \pm 3°$. The contact angle of M21 (oxidized MWCNT-incorporated mixed-matrix membranes) is $65.3 \pm 2°$, indicating the most hydrophilic surface. Such a decrease in the contact angle could be the indication of the

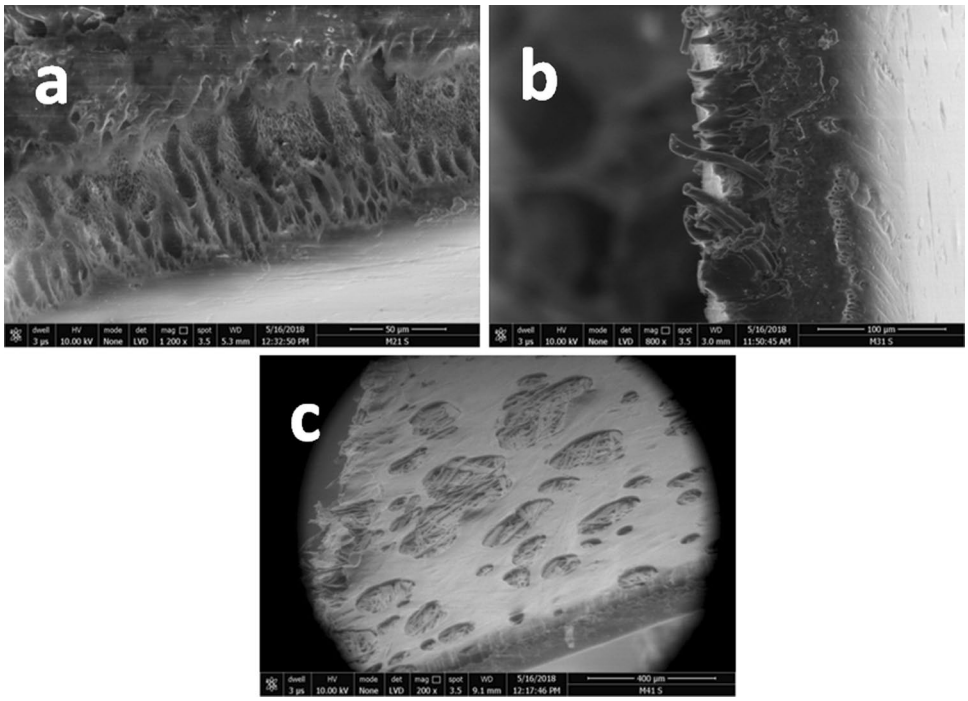

Fig. 1 SEM micrograph of cross section of cold-fractured membranes **a** M21, **b** M31, **c** M41

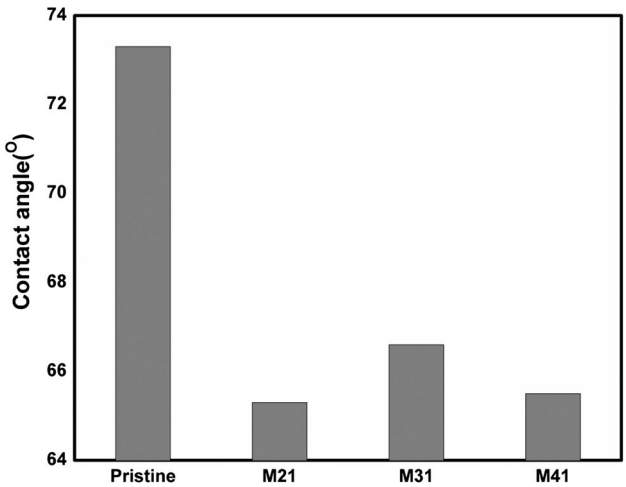

Fig. 2 Contact angle of pristine PES as compared nanotube-incorporated membranes

Table 2 Variation of pore diameter and required pressure for different concentration of MWCNT

Parameter	M31	M41
Mean flow pore pressure (psi)	48.7	50.6
Mean flow pore diameter (μ)	0.13	0.13
Bubble point pressure (psi)	45.3	50.6
Bubble point diameter (μ)	0.14	0.13

presence of functionalized nanotubes in the PES matrix as well as the indication of well aligned MWCNT structure in the membrane matrix.

The membranes having nanotubes could pass the water much smoothly which is supported by the enhanced pure water flux of mixed-matrix membranes. Mercury flow porosimeter analysis reveals the pore dimensions of the membranes. The study shows the dimensions of the pore size of polymer vary with the addition of MWCNT in the membranes. The largest pore of the membranes was detected by bubble point diameter as by applying the pressure the pores are emptied the Mercury fluid. The fluid was removed from the other smaller pores on application of higher pressure. The bubble point pressure obtained for azide-functionalized MWCNT-incorporated mixed-matrix membranes is 50.64 psi, and bubble point diameter obtained is 0.13 μ. The data are summarized in Table 2.

On comparing the mean flow pore pressure and bubble point pressure of the azide- and amide-functionalized nanotube-incorporated mixed-matrix membranes, the pressure applied to empty the mercury fluid is higher in case of azide, hence smaller pore size, which is in agreement with the SANS results. Detailed structural information of the inorganic filler-incorporated polymeric membranes was studied by the neutron scattering technique namely small-angle neutron scattering (SANS). The data are interpreted using SASFIT software. Throughout the data analysis, corrections were made for instrumental smearing. The calculated scattering profiles were smeared by the appropriate resolution function to compare with the measured data.

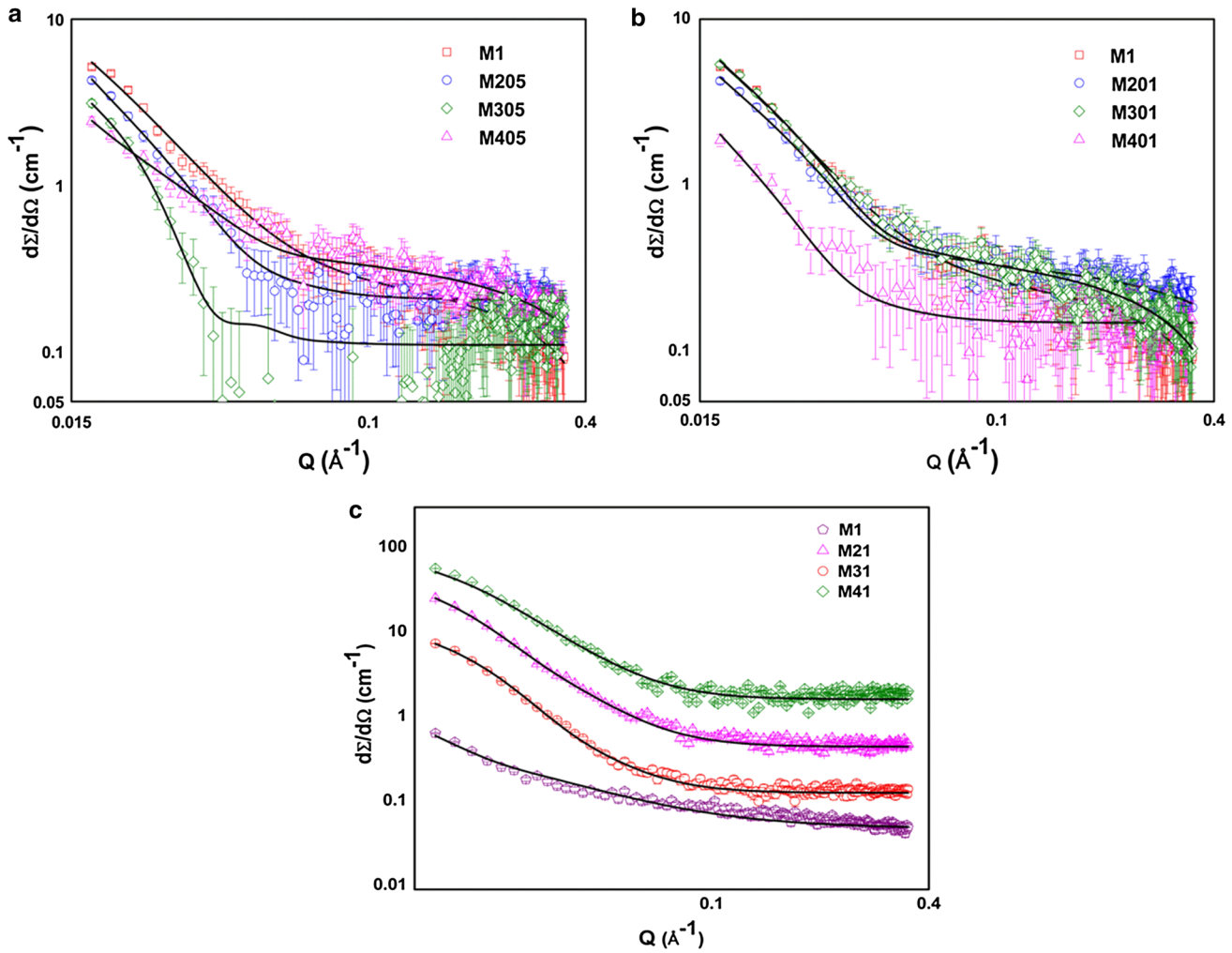

Fig. 3 SANS profile of membrane soaked in D_2O **a** 0.05 wt% nanotubes, **b** 0.1 wt% nanotubes, **c** 1.0 wt% nanotubes

Figure 3 shows the SANS data of the pure as well as functionalized membranes soaked in the D_2O. The scattering intensities for the different membrane samples are presented and shifted vertically for the clarity of the presentation. There are two models that are considered: (1) the polydispersed sphere model where the pores are considered to be spherical and surrounded by a matrix material and (2) the random two-phase model, where first phase is the pores and the second phase the surrounding matrix material.

Our data were better fit to the second model which shows that there is presence of nanotubes within the pores. The correlation length is found to be 3.9 nm in the pristine PES membrane as well as in the mixed-matrix membrane containing 1 weight percentage of MWCNT and in the membranes containing smaller percentage of nanotubes the value is about 4.8 nm. As it is the most repeated distance between the pores and is same for both pristine and mixed-matrix membrane, however, pore radius is decreased in later case which implies that porosity of the membrane is increased with the addition of the 1 weight percentage of nanotubes which is in agreement with enhanced porosity of membranes containing nanotubes reported in our previous work (Gupta et al. 2015) (Fig. 4). However, lower percentage of addition of nanotubes does not affect the porosity. The addition of the CNTs influences the SANS data in the intermediate Q range. All these data have been analyzed by considering the scattering contributions from the CNTs along with that from the distributed pores. The CNT radius is found to be about

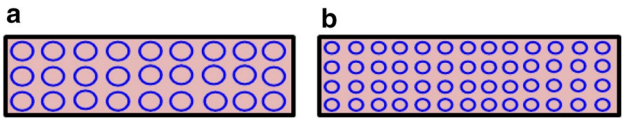

Fig. 4 Schematic representation of arrangement of pores in **a** pristine membrane and **b** mixed-matrix membrane. The pores in **a** are larger that the pores in **b** even though the correlation length, i.e., the distance between the pores remains the same

4 nm, while the length of the CNTs (in microns) cannot be estimated due to the limited Q range of the data. The fitted parameters are listed in Table 3.

Rejection performance of heavy metals

The stock solutions for the separation experiment were prepared by dissolving the appropriate amount of salts in deionized water (1000 ppm). The tests were carried out to study the rejection performance of chromium, lead, cadmium, copper, and arsenic heavy metals by the prepared mixed-matrix and polymeric PES membranes. We have performed experiment for the pure water flux and rejection at two different pressures (71 psi and 98 psi) and at acidic as well as neutral pH for chromium metals and at optimum condition (71 psi and 2.5 pH) for rest of the metals. The effect of pH and pressure on rejection is shown in Figs. 5 and 6, respectively, for the azide-functionalized MWCNT-incorporated mixed-matrix membranes. As shown in Fig. 5 at acidic pH, the rejection is higher and this may be due to that the proton also competes with heavy metal at acidic pH which is not in case of neutral pH. However, the reason behind the lower rejection on increasing the pressure could be the enhanced flux of the membranes at higher pressure (Fig. 7) and compaction of the membranes. The effect of pressure on values of the pure water flux (L/m^{2}h) is shown in Table 4.

The rejection percentage of Cr(VI), Pb(II), and Cu(II) is 74.0, 69.2, and 92.5, respectively, at 71 psi (2.5 pH) for azide membrane having 1% MWCNT concentration which is decreased to 52.3, 31.2, and 80.5 at higher pressure. At similar conditions, the rejection percentage of Cr(VI), Pb(II), and Cu(II) is 63.1, 55.3, 86.7, and 46.1, 42.7, and 52.3 for 0.1% and 0.05% concentration, which is reduced to 42.3, 35.7, 70.1 and 36.2, 30.4, 34.3, respectively, on increasing the pressure applied to the membranes. All the values are summarized in Table 5. As shown in Table 4, the pure water flux for mixed-matrix membrane having MWCNT percentage 0.05 is higher than 1; however, the rejection capacity of membrane having higher nanotube concentration is more (Fig. 8). The higher flux accounts for the lesser hindrance at the surface of the membranes due to lesser percentage of nanotubes as well as bigger pores compared to membranes containing higher weight percentage nanotubes, thus resulting in lesser rejection comparatively.

Table 3 SANS data of membrane soaked in D_2O containing different concentration of MWCNT, M1 (pristine), M205; M201; M21 (oxidized), M305; M301; M31 (amide), M405; M401; M41 (azide)

Sample	Pore radius (nm)	Polydispersity (σ)	Correlation length (nm)
M1	14.8	0.27	3.9
M205	10.9	0.20	4.8
M201	13.0	0.20	4.8
M21	9.7	0.27	3.9
M305	9.1	0.20	4.9
M301	14.0	0.20	4.9
M31	8.3	0.29	3.9
M405	11.0	0.20	4.9
M401	10.5	0.20	4.9
M41	7.4	0.27	3.9

It may be pointed out that the distribution of the pores does not change with addition of the CNTs while the pore radius reduces significantly

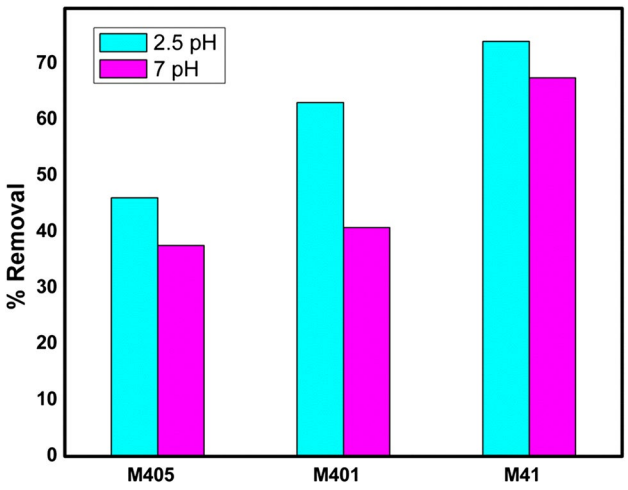

Fig. 5 Percentage removal of Cr(VI) metal ion at acidic and neutral pH for different mixed-matrix azide-functionalized MWCNT/PES membranes at 71psi pressure

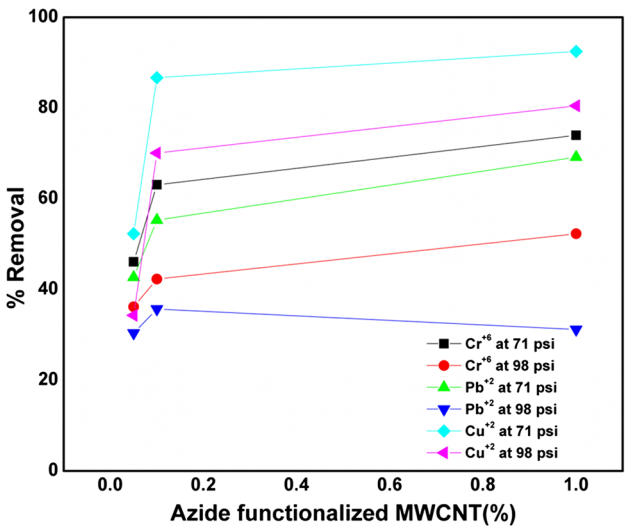

Fig. 6 Percentage rejection of metal ions at pH 2.5 for mixed-matrix azide-functionalized MWCNT/PES membranes containing different percentage of nanotubes at different pressure

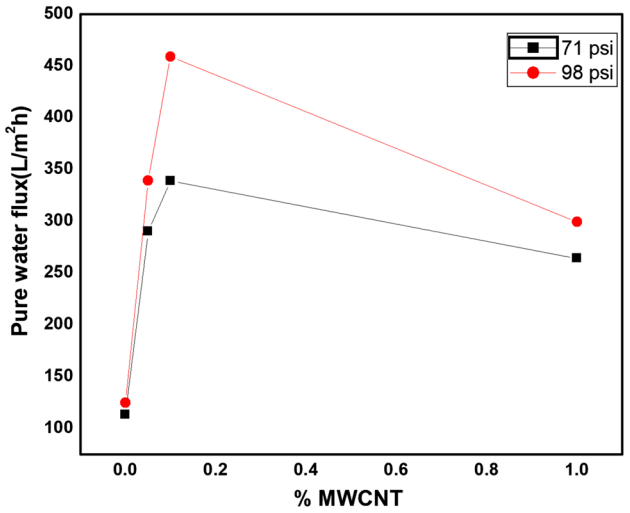

Fig. 7 Pure water flux of azide-functionalized MWCNT/PES membranes containing different % of nanotubes at different pressure

Table 4 Variation of pure water flux of membranes with pressure

Membrane	Pure water flux (L/m^2h)	
	71 psi	98 psi
M1	113	124
M205	108	158
M201	431	480
M21	306	373
M305	294	347
M301	343	461
M31	293	327
M405	290	339
M401	339	459
M41	264	299

Our mixed-matrix membranes are giving very highly pure water flux (around 450 LMH) which clearly shows that the water preferentially goes through the nanotubes present in the pore and, because of the hydrophobic walls of nanotubes, the flow is much smoother which is not in case of pristine PES membrane. From the experiments, we have found the optimum condition for rejection studies is at pH 2.5 and 71 psi pressure.

The rejection experiments were performed at the above-mentioned optimum condition (pH 2.5 and pressure 71 psi) for pristine PES, oxidized, azide- and amide-functionalized MWCNT-incorporated mixed-matrix membranes. It is observed from the data shown in Tables 6, 7, and 8 that nanotube-incorporated membranes are having better rejection than pristine PES membrane which is because of the presence of functionalized nanotube and they not only reduce the pore size of the membranes but also smoothen the path of water inside the pores, hence resulting in better rejection. The attached functionalities –COOH, –CONHCH$_2$CH$_2$NH$_2$, and –CON$_3$ enable the complexation ability of the membranes with heavy metal ions. Among all the three functionalities, azide-functionalized membranes are giving the best rejection which is due to higher metal-binding capacity of azide functional group. The maximum rejection is obtained at acidic pH because protons also compete with the heavy metal ions.

Conclusions

This study reports the mixed-matrix membranes with higher flux which is due to the better interaction of the functionalized nanotubes and polymer matrix as well as frictionless transport of water through nanotube channels. The nanotubes facilitate the ease of flowing water through the linked channels resulting in higher rejection as well as enhanced pure water flux. The azide-functionalized nanotubes as fillers provide best results for the removal of toxic metals Cu(II), As(III), Cd(II), Cr(VI), and Pb(II). We get the highest rejection of Cu(II), i.e., 92.1% from 1 wt% concentration of azide-functionalized MWCNT/PES mixed-matrix membranes, among all the above-mentioned heavy metals. However, the work regarding the mechanism of membrane filtration performance is in progress.

Table 5 Rejection studies of metal ions at pH 2.5 for azide-functionalized MWCNT/PES membranes at pressure 71 psi and 98 psi

Membrane	Removal capacity (%)					
	Cr(VI)		Pb(II)		Cu(II)	
	71 psi	98 psi	71 psi	98 psi	71 psi	98 psi
M1	20.0	17.1	19.0	16.3	22.9	21.3
M405	46.1	36.2	42.7	30.4	52.3	34.3
M401	63.1	42.3	55.3	35.7	86.7	70.1
M41	74.0	52.3	69.2	31.2	92.5	80.5

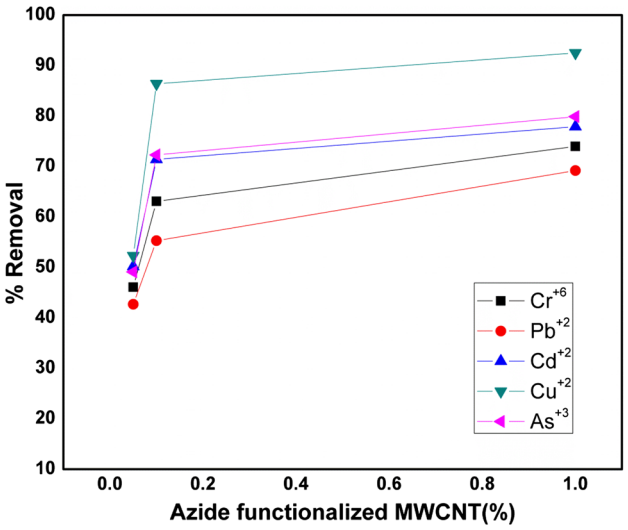

Fig. 8 Percentage rejection of metal ions at pH 2.5 for mixed-matrix azide-functionalized MWCNT/PES membranes containing different % of nanotubes at 71 psi pressure

Table 6 Rejection studies of heavy metal ions at pH 2.5 for oxidized MWCNT/PES membranes at pressure of 71 psi

Membrane	Removal capacity (%)				
	Cr(VI)	Pb(II)	Cd(II)	Cu(II)	As(III)
M1	20.0	19.0	20.5	22.9	18.3
M205	31.1	22.3	49.7	45.5	51.2
M201	49.3	29.1	54.3	48.2	55.3
M21	58.5	35.5	68.1	78.3	75.7

Table 7 Rejection studies of heavy metal ions at pH 2.5 for amide-functionalized MWCNT/PES membranes at pressure of 71 psi

Membrane	Removal capacity (%)				
	Cr(VI)	Pb(II)	Cd(II)	Cu(II)	As(III)
M1	20.0	19.0	20.5	22.9	18.3
M305	45.3	43.2	49.2	50.3	51.2
M301	62.2	54.7	75.1	85.1	74.9
M31	73.5	68.7	79.5	92.1	80.3

Table 8 Rejection studies of heavy metal ions at pH 2.5 for azide-functionalized MWCNT/PES membranes at pressure of 71 psi

Membrane	Removal capacity (%)				
	Cr(VI)	Pb(II)	Cd(II)	Cu(II)	As(III)
M1	20.0	19.0	20.5	22.9	18.3
M405	46.1	42.7	50.2	52.3	49.1
M401	63.1	55.3	71.4	86.4	72.3
M41	74.0	69.2	77.9	92.5	79.9

Acknowledgements This work was supported by UGC-DAE [Grant CRS-M-193]. There is no conflict of interest among the authors.

References

Adams FV, Nxumalo EN, Krause RMW, Hoek EMV, Mamba BB (2014) Application of polysulfone/cyclodextrin mixed-matrix membranes in the removal of natural organic matter from water. J Phys Chem Earth 67–69:71–78

Ahmad AL, Abdulkarim AA, Shafie ZMHM, Ooi BS (2017) Fouling evaluation of PES/ZnO mixed matrix hollow fiber membrane. Desalination 403:53–63

Alam J, Dass LA, Ghasemi M, Alhoshan M (2013) Synthesis and optimization of PES–Fe_3O_4 mixed matrix nanocomposite membrane: application studies in water purification. J Membr Sci 34:1870–1877

Amiri F, Moghadassi AR, Bagheripour E, Parvizian F (2017) Fabrication and characterization of PES based nanofiltration membrane modified by zeolite nanoparticles for water desalination. J Membr Sci Res 3:50–56

Aswal VK, Goyal PS (2000) Small-angle neutron scattering diffractometer at Dhruva reactor. Curr Sci 79:947–953

Bagheripour E, Moghadassi AR, Hosseini SM, Nemati M (2016) Fabrication and characterization of novel mixed matrix polyethersulfone nanofiltration membrane modified by iron-nickel oxide nanoparticles. J Membr Sci Res 2:14–19

Benally C, Li M, El-Din MG (2018) The effect of carboxyl multiwalled carbon nanotubes content on the structure and performance of polysulfone membranes for oil sands process-affected water treatment. Sep Purif Technol 199:170–181

Celik E, Liu L, Choi H (2011a) Protein fouling behavior of carbon nanotube/polyethersulfone composite membranes during water filtration. Water Res 45:5287–5294

Celik E, Park H, Choi H, Choi H (2011b) Carbon nanotube blended polyethersulfone membranes for fouling control in water treatment. Water Res 45:274–282

Chai PV, Mahmoudi E, Teow YH, Mohammad AW (2017) Preparation of novel polysulfone–Fe_3O_4/GO mixed-matrix membrane for humic acid rejection. J Water Process Eng 15:83–88

Chan KH, Wong ET, Idris A, Yusof NM (2015) Modification of PES membrane by PEG-coated cobalt doped iron oxide for improved Cu(II) removal. J Ind Eng Chem 27:283–290

Delavara M, Bakeri Gh, Hosseini M (2017) Fabrication of polycarbonate mixed matrix membranes containing hydrous manganese oxide and alumina nanoparticles for heavy metal decontamination: characterization and comparative study. Chem Eng Res Des 120:240–253

Elizalde CNB, Al-Gharabli S, Kujawa J, Mavukkandy M, Hasan SW, Arafat HA (2018) Fabrication of blend polyvinylidene fluoride/chitosan membranes for enhanced flux and fouling resistance. Sep Purif Technol 190:68–76

Esfahani MR, Tyler JL, Stretz HA, Wells MJM (2015) Effects of a dual nanofiller, nano-TiO_2 and MWCNT, for polysulfone-based nanocomposite membranes for water purification. Desalination 372:47–56

Farahani MHDA, Vatanpour V (2018) A comprehensive study on the performance and antifouling enhancement of the PVDF mixed

matrix membranes by embedding different nanoparticulates: clay, functionalized carbon nanotube, SiO_2 and TiO_2. Sep Purif Technol 197:372–381

Ghaemi N, Madaeni SS, Daraei P, Rajabi H, Zinadini S, Alizadeh A, Heydari R, Beygzadeh M, Ghouzivand S (2015) Polyethersulfone membrane enhanced with iron oxide nanoparticles for copper removal from water: application of new functionalized Fe_3O_4 nanoparticles. Chem Eng J 263:101–112

Goh PS, Ismail AF, Ng BC (2013) Carbon nanotubes for desalination: performance evaluation and current hurdles. Desalination 308:2–14

Gohari RJ, Halakoo E, Nazri NAM, Lau WJ, Matsuura T, Ismail AF (2014) Improving performance and antifouling capability of PES UF membranes via blending with highly hydrophilic hydrous manganese dioxide nanoparticles. Desalination 335:87–95

Grabczyk AW, Kubica P, Jankowski A, Wojtowicz M, Kansy J, Wojtyniak M (2017) Gas and water vapor transport properties of mixed matrix membranes containing 13X zeolites. J Membr Sci 526:334–347

Gupta S, Bhatiya D, Murthy CN (2015) Metal removal studies by composite membrane of polysulfone and functionalized single-walled carbon nanotubes. Sep Sci Technol 50:421–429

Ho KC, Teow YH, Ang WL, Mohammad AW (2017) Novel GO/OMWCNTs mixed-matrix membrane with enhanced antifouling property for palm oil mill effluent treatment. Sep Purif Technol 177:337–349

Hosseini SS, Nazif A, Di MAAS, Ortiz I (2017) Fabrication, tuning and optimization of poly (acrilonitryle) nanofiltration membranes for effective nickel and chromium removal from electroplating wastewater. Sep Purif Technol 187:46–59

Huang J, Shu Z, Zhang Y (2017) Fabrication and performance of a polyethersulfone nanofiltration membrane impregnated with a mesoporous silica–poly(1-vinylpyrrolidone) nanocomposite. Polym Compos 38:908–917

Karim AA, Leaper S, Alberto M, Vijayaraghavan A, Fan X, Holmes SM, Souaya ER, Badawy MI, Gorgojo P (2017) High flux and fouling resistant flat sheet polyethersulfone membranes incorporated with graphene oxide for ultrafiltration applications. Chem Eng J 334(2017):789–799

Karkooti A, Yazdi AZ, Chen P, McGregor M, Nazemifard N, Sadrzadeh M (2018) Development of advanced nanocomposite membranes using graphene nanoribbons and nanosheets for water treatment. J Membr Sci 560:97–107

Kim ES, Hwang G, Din MGE, Liu Y (2012) Development of nanosilver and multi-walled carbon nanotubes thin-film nanocomposite membrane for enhanced water treatment. J Membr Sci 394–395:37–48

Kim HJ, Choi K, Baek Y, Kim DG, Shim J, Yoon J, Lee JC (2014) High-performance reverse osmosis CNT/Polyamide nanocomposite membrane by controlled interfacial interactions. ACS Appl Mater Interfaces 6:2819–2829

Lee J, Ye Y, Ward AJ, Zhou C, Chen V, Minett AI, Lee S, Liu Z, Chae S, Shi J (2016) High flux and high selectivity carbon nanotube composite membrane for natural organic matter removal. Sep Purif Technol 163:109–119

Liu F, Ma BR, Zhou D, Xiang YH, Xue LX (2014) Breaking through tradeoff of polysulfone ultrafiltration membranes by zeolite 4A. Microporous Mesoporous Mater 186:113–120

Liu Z, Mi Z, Jin S, Wang C, Wang D, Zhao X, Zhou H, Chen C (2018) The influence of sulfonated hyperbranched polyethersulfone-modified halloysite nanotubes on the compatibility and water separation performance of polyethersulfone hybrid ultrafiltration membranes. J Membr Sci 557:13–23

Luo ML, Zhao JQ, Tang W, Pu CS (2005) Hydrophilic modification of poly(ether sulfone) ultrafiltration membrane surface by self-assembly of TiO_2 nanoparticles. App Surf Sci 249:76–84

Mangukiya S, Prajapati S, Kumar S, Aswal VK, Murthy CN (2016) Polysulfone-based composite membranes with functionalized carbon nanotubes show controlled porosity and enhanced electrical conductivity. J Appl Polym Sci 133:43778

Martín A, Arsuaga JM, Roldán N, Martínez A, Sotto A (2016) Effect of amine functionalization of SBA-15 used as filler on the morphology and permeation properties of polyethersulfone-doped ultrafiltration membranes. J Membr Sci 520:8–18

Mavukkandy MO, Bilad MR, Kujawa J, Al-Gharabli S, Arafat HA (2017) On the effect of fumed silica particles on the structure, properties and application of PVDF membranes. Sep Purif Technol 187:365–373

Mbuli B, Mahlambi M, Ngila CJ, Moutloali R (2018) Polysulfone ultrafiltration membranes modified with carbon-coated alumina supported Ni–TiO_2 nanoparticles for water treatment: synthesis, characterization and applications. J Membr Sci Res. https://doi.org/10.22079/jmsr.2018.80046.1173

Mondal M, Dutta M, De S (2017) A novel ultrafiltration grade nickel iron oxide doped hollow fiber mixed matrix membrane: spinning, characterization and application in heavy metal removal. J Sep Purif 188:155–166

Mukherjee R, Bhunia P, De S (2016) Impact of graphene oxide on removal of heavy metals using mixed matrix membrane. Chem Eng J 292:284–297

Munnawar I, Iqbal SS, Anwar MN, Batool M, Tariq S, Faitma N, Khan AL, Khan AU, Nazar U, Jamil T, Ahmad NM (2017) Synergistic effect of chitosan-zinc oxide hybrid nanoparticles on antibiofouling and water disinfection of mixed matrix polyethersulfone nanocomposite membranes. Carbohydr Polym 175:661–670

Pedersen JS (1997) Analysis of small-angle neutron scattering data from colloids and polymer solutions: modeling and least-square fitting. Adv Colloid Interface Sci 70:171

Qiu S, Wu L, Pan X, Zhang L, Chen H, Gao C (2009) Preparation and properties of functionalized carbon nanotube/PSF blend ultrafiltration membranes. J Membr Sci 342:165–172

Rahimpour A, Jahanshahi M, Mollahosseini A, Rajaeian B (2012) Structural and performance properties of UV-assisted TiO_2 deposited nano-composite PVDF/SPES membranes. Desalination 285:31–38

Shah P, Murthy CN (2013) Studies on the porosity control of MWCNT/polysulfone composite membrane and its effect on metal removal. J Membr Sci 437:90–98

Sonawane SH, Terrien A, Figueiredo AS, Goncalves MC, Pinho MND (2017) The role of silver nanoparticles on mixed matrix Ag/cellulose acetate asymmetric membranes. Polym Compos 38:32–39

Taurozzi JS, Arul H, Bosak VZ, Burban AF, Voice TC, Bruening ML, Tarabara VV (2008) Effect of filler incorporation route on the properties of polysulfone silver nanocomposite membranes of different porosities. J Membr Sci 325:58–68

Yin J, Zhu J, Deng B (2013) Multiwalled carbon nanotubes (MWNTs)/polysulfone (PSU) mixed matrix hollow fiber membranes for enhanced water treatment. J Membr Sci 437:237–248

Zhang M, Zhang K, Gusseme BD, Verstraete W (2012) Biogenic silver nanoparticles (bio-Ag0) decrease biofouling of bio-Ag0/PES nanocomposite membranes. Water Res 46:2077–2087

Zhang Y, Zhao J, Chu H, Zhou X, Wei Y (2014) Effect of modified attapulgite addition on the performance of a PVDF ultrafiltration membrane. Desalination 344:71–78

Zhang H, Guo R, Hou J, Wei Z, Li X (2016) Mixed matrix membranes containing carbon nanotubes composite with hydrogel for efficient CO_2 separation. ACS Appl Mater Interfaces 8:29044–29051